

Characterization of Clay Raw Materials from Three Kankan Clay Deposits with a View to Their Use as Building Materials

Thierno Abdoulaye Barry^{1,2*}, Abdou Mbaye¹, Insa Badiane¹, Albert Manga Badiane¹, Stéphane Freslon³, Bérenger Aranda⁴, Laurent Molez⁴, Magatte Camara¹

¹Laboratoire de Chimie et physique des Matériaux (LCPM), UFR des Sciences Techniques et Ingénierie (STI) de l'Université Assane Seck de Ziguinchor (UASZ), Ziguinchor, Sénégal

²Laboratoire de Chimie Analytique, Département de Chimie, Université Gamal Abdel Nasser de Conakry, Conakry, Guinée

³Laboratoire de Chimie du solide et Matériaux, Institut des Sciences Chimiques de Rennes, Coësmes, France

⁴Laboratoire de Génie Civil et Génie Mécanique (LGCGM) de l'Institut National des Sciences Appliquées de Rennes, Coësmes, France

Email: *ta.b1@zig.univ.sn, abdou.mbaye@univ-zig.sn, magatte.camara@univ-zig.sn

How to cite this paper: Barry, T.A., Mbaye, A., Badiane, I., Badiane, A.M., Freslon, S., Aranda, B., Molez, L. and Camara, M. (2025) Characterization of Clay Raw Materials from Three Kankan Clay Deposits with a View to Their Use as Building Materials. *Journal of Materials Science and Chemical Engineering*, 13, 31-52.

<https://doi.org/10.4236/msce.2025.132003>

Received: January 8, 2025

Accepted: February 17, 2025

Published: February 20, 2025

Copyright © 2025 by author(s) and Scientific Research Publishing Inc.

This work is licensed under the Creative Commons Attribution International License (CC BY 4.0).

<http://creativecommons.org/licenses/by/4.0/>



Open Access

Abstract

Clays are a constituent of the earth. As a result, the discovery and traditional use of clays in construction and pottery worldwide dates back to antiquity. Guinea has several deposits of clay minerals whose chemical and mineralogical compositions have been little studied. Despite lacking of scientific data on these clay minerals, they are used today in pottery and habitat construction. As a step towards promoting the use of clay materials in Guinea, we conducted a study of the physicochemical and mineralogical properties of three natural clays from Kakan in the Republic of Guinea (AKKB, AKKE, AKKO) used in habitat construction. The aims of this work were to better understand their properties, but above all to be able to act on them to improve and broaden their applications, which until now have been limited to construction. These clays were studied by X-ray diffraction (XRD), X-ray fluorescence spectrometry (XRF), moisture content (%W), laser granulometry, Atterberg limits, specific surface area, infrared spectroscopy (FT-IR), scanning electron microscopy (SEM), thermogravimetric analysis and differential thermal analysis (TGA/DTA). These analyses revealed that the main clay minerals present in our samples are kaolinite, illite and, montmorillonite, with the addition of impurities, the most abundant of which is quartz.

Keywords

Characterization, Clay Minerals, Kankan, Habitat Construction

1. Introduction

Clay science is a pluridisciplinary field that brings together researchers from a variety of specialities (geology, mineralogy, cristallography, chemistry and geotechnics), with different objectives in mind [1] [2].

Interest in this field has been growing recently as its industrial applications continue to diversify. Clay is the oldest mineral used by man in pottery and habitat construction [2].

The term “clay” has been defined as a natural material composed mainly of fine-grained minerals (clay minerals), generally plastic at appropriate water contents and hardening when dried or fired [3].

The discovery and traditional use of clay materials dates back to antiquity throughout the world: in Africa (Egypt), the Middle East (Turkey), Asia (China), America (Mexico), Europe (Rome), etc. [4].

In recent years, clay, which had been abandoned in favor of cement, has enjoyed renewed interest thanks to its availability, reduced ecological impact and hygroscopic and thermal properties [5].

In several sub-Saharan African countries, including Burkina Faso and Guinea, numerous studies are being carried out to evaluate the properties of clay as a raw material for eco-construction [6] [7].

As for the Republic of Guinea, it abounds in large deposits of useful minerals such as clays, sand, granite, laterite, limestone, etc. [8]; some of which are traditionally exploited by communities. Clays, long neglected after the discovery of hydraulic binders and their derivatives, are now used throughout Guinea in the habitat sector, particularly in Kankan.

This widespread use of clay in housing construction in the city of Kankan is justified on the one hand by a demographic increase from 392.768 inhabitants (10.7%) in 2014 to 472.505 inhabitants (10.9%) in 2019 [9], making it the 3rd most populous city in the country after the capital Conakry and Kindia, and on the other hand by the high cost of hydraulic binders. Added to this is the environmental problem caused by the pollution generated by the production of these materials known as hydraulic binders.

Integrating these clay materials into the construction of decent, accessible and sustainable housing, infrastructure and facilities is therefore a crucial challenge on an international scale.

Against this backdrop of high building material prices, sustainable development, and technological innovation in the field of research, clays offer a viable alternative for a wide variety of applications.

Earth used in construction requires sufficient cohesion, provided by the clay

that acts as a natural binder [5].

The use of clays is intrinsically linked to knowledge of their properties, which is why we have undertaken the physicochemical, mineralogical and geotechnical characterization of clay raw materials from three clay deposits in Kankan (Republic of Guinea) with a view to their use as building materials.

2. Materials and Methods

2.1. Study Area

The Kankan area is located in the north-east of the Republic of Guinea, 635 km from the capital Conakry. Its surface area is approximately 72,145 km² with a population of 472,505 habitants in 2019 [9]. In geographical coordinates, it extends from 10°23' North latitude and 9°18' West longitude. See **Figure 1**, which shows the map of Kankan and its position within the Republic of Guinea.

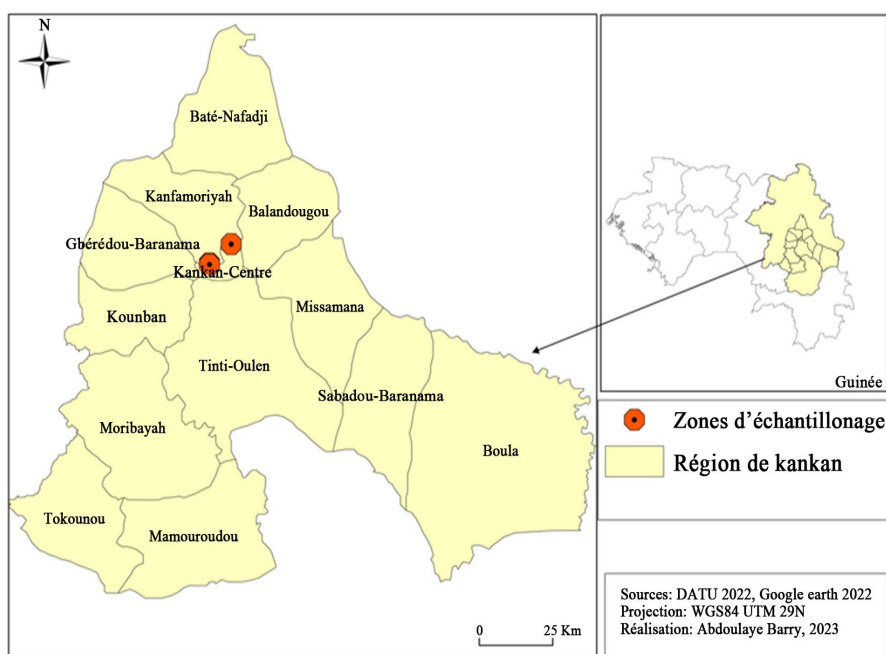


Figure 1. Map of the Kankan region showing sampling zones [10].

2.2. Geological Setting

Guinea's geology is dominated by Paleozoic terrains with Mesozoic zones. In the northeastern region around Kankan, Proterozoic facies predominate, alternating with Archean formations [11] [12].

The Kankan region has a varied geology:

Lower Proterozoic: Mainly present, with sedimentary and effusive layers.

Upper Proterozoic: Located in the northwest, composed of sandstones and conglomerates, forming plateaus bordered by cliffs.

Paleozoic: Outcrops to the north, with a base of quartz conglomerates resting on Proterozoic granites [13].

2.3. Sample Collection and Preparation

Clay samples were taken from representative areas to accurately reflect local geological and mineralogical characteristics. Samples were taken at depths of 1 m (AKKB), 3 m (AKKE) and 3 m (AKKO) to study depth-related variations. A quantity of 5 kg per site was collected to enable in-depth analysis.

The Process used appropriate tools, including a geological map, shovel, spatula, hammer, bags, GPS, labels and marker. Each sample was labelled with precise information (date, location and coordinates). Samples were packaged in airtight plastic bags to preserve their physical and chemical properties.

For the present work, we took three clay samples from the areas deemed to be the most exploited in Kankan. The samples were taken in such a way as to be able to characterize both the clays from the Balandougou Sub-Prefecture (AKKB) and the clays from the Energie (AKKE) and Kankankoura (AKKO) urban districts.

Table 1 shows the clay sampling areas and their geographical coordinates.

Table 1. Sampling of Kankan clays.

Area	Sampling zone	N	W	
Kankan	Sub-Prefecture of Balandougou	10°36'08.7"	_ 09°30'15.5"	
		10°39'44.9"	_ 09°26'98.5"	
	Kankankoura district	10°36'11.3"	_ 09°30'15.2"	
		10°36'68.4"	_ 09°28'70.2"	
		Energie district	10°36'08.7"	_ 09°01'55.0"
			10°36'15.4"	_ 09°30'13.1"

2.4. Analytical Methods and Materials

2.4.1. Moisture Content

The moisture content of clays was determined using a “Despatch 2000” oven calibrated at 105°C.

The following formula was used to calculate the natural moisture content (%W):

$$\%W = \frac{P_1 - P_2}{P_e} \times 100 \quad (1)$$

P_1 : weight of bin plus sample before drying.

P_2 : weight of bin plus sample after drying.

P_e : test plug weight.

2.4.2. Mineralogical Analysis

Mineralogical phases were identified using a Panalytical X'Pert Pro diffractometer equipped with an X' Celerator detector. Experimental conditions were as follows: Cu K α radiation ($\lambda = 1.542 \text{ \AA}$), I = 40 mA, V = 45 kV. Peaks were identified using X'Pert HighScore software.

2.4.3. Characterization Techniques

Chemical composition in terms of major oxides was determined by X-ray fluorescence spectrometry (XRF). This analysis was carried out using the “AXIOS FAST,

PANalytical 206204" instrument.

2.4.4. FTIR Spectroscopy

FT-IR measurements were carried out on a Perkin Elmer Frontier spectrometer using the UATR (Universal Attenuated Total Reflectance) accessory. Spectra were recorded between 650 and 4000 cm^{-1} , on the clay samples.

2.4.5. Physical Properties

The Atterberg limit is determined by the falling cone method, which measures the penetration of the cone into the soil after release, with better resolution.

The Malvern Mastersizer 2000 manufactured by Malvern Instruments was used as a laser particle analyzer for clays. This device works on the basis of Mie theory to obtain particle size distribution by converting light-scattering data.

The specific surface area was measured using a Dewar "vacprep 061" gas vacuum spectrometer coupled to a TriStar II Plus Porosimeter.

2.4.6. Morphological Study

SEM images were obtained with a Hitachi TM 1000 tabletop microscope, version 02.11 (Hitachi High Technologies, Corporation Tokyo Japan). Samples were assembled on carbon disks, glued to a carbon stub. The reproducibility of the elemental analyses was checked by repeating the measurements several times for several spots per sample.

2.4.7. Thermal Analysis

Thermal analyses were carried out with a Perkin Elmer Pyris Diamond ATG/ATD analyzer between room temperature and 950 °C at a rate of 5 °C/minute in platinum crucibles under a nitrogen atmosphere. Compounds were held for 1 hour at 950 °C in an air atmosphere to ensure complete combustion.

3. Results and Discussion

3.1. Structural Analysis

3.1.1. Phase Identification

X-ray diffraction patterns for the three clays AKKB, AKKE, and AKKO are shown in **Figure 2**. The main lines observed on the diffractogram of the clay fraction are attributed to kaolinite ($\text{Al}_2\text{Si}_2\text{O}_5(\text{OH})_4$), illite[(K, H_3O) $\text{Al}_2\text{Si}_3\text{AlO}_{10}(\text{OH})_2$], and montmorillonite (bentonite) [(Na, Ca) $_{0.3}(\text{Al}, \text{Mg})_2\text{Si}_4\text{O}_{10}(\text{OH})_{2x}\text{H}_2\text{O}$]. These raw samples also contain quartz (SiO_2), magnetite (Fe_3O_4), and, in smaller proportions, muscovite [(K, NH_4 , Ca) $\text{Al}_2(\text{Si}, \text{Al})_4\text{O}_{10}(\text{OH})_2$], gibbsite [$\text{Al}(\text{OH})_3$] in sample AKKE, and feldspar such as microcline (KAlSi_3O_8) in sample AKKB. Clinocllore [($\text{Mg}_5\text{Al}(\text{Si}_3\text{Al})\text{O}_{10}(\text{OH})_8$)] is also present, except in sample AKKE, which is not as similar in mineralogical composition to the other two samples. The relatively high intensity of quartz peaks in all samples indicates a significant presence of free silica. This can be confirmed by a higher $\text{SiO}_2/\text{Al}_2\text{O}_3$ ratio (2.61 to 3.45) and lower loss on ignition [14].

The presence of illite in clays can lead to the formation of a glassy phase and

lower the melting point while reducing linear shrinkage and the formation of cristobalite and mullite. Clinocllore, one of the most abundant elements in the chlorite group, is composed mainly of magnesium, with moderate amounts of silicon, aluminum, and iron. Iron oxidation in clinocllore gives it an attractive appearance, making AKKB and AKKO clays suitable for decorative and sculptural stones. They can also be used to prepare bricks for exterior walls for aesthetic purposes [15].

The clays mainly reveal the presence of two intense peaks, one corresponding to Quartz and the other to a mixture of Kaolinite, illite, and Montmorillonite sometimes stratified with illite, magnetite, and muscovite, implying that our clay is heterogeneous. This confirms the results of the particle size distribution, which shows bimodal forms, especially on AKKB and AKKE.

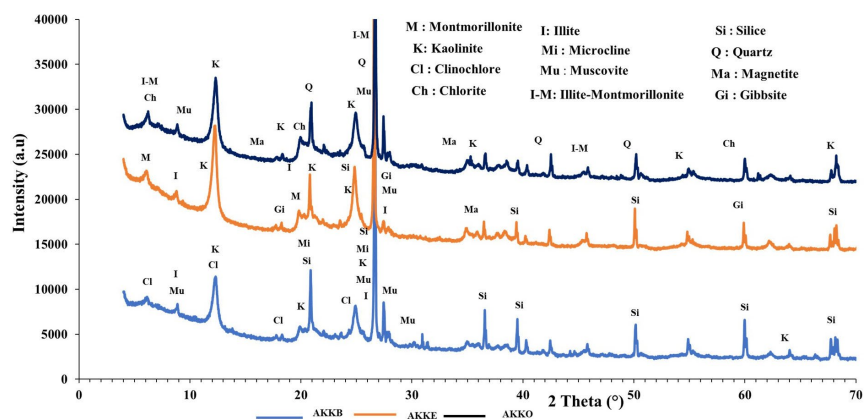


Figure 2. Diffractograms of Kankan natural clays.

The existence of peaks from the smectite group implies further treatments of our clays, namely solvating with glycerol and heating to 550 °C, to obtain more precision on their mineralogical composition.

The reflection peaks of kaolinite, visible at around 12.29 Å and 26.57 Å, remained unchanged when the samples were solvated with glycerol, but disappeared when heated to 550 °C due to structural destruction. This behavior is characteristic of kaolinite (Hong *et al.*, 2012; Tsao *et al.*, 2013).

The presence of illite is confirmed by reflection peaks at 8.76 Å and 26.57 Å, which remained unchanged when the samples were subjected to glycolation and heat treatment at 550 °C.

Peaks of non-clay minerals, such as silica, were recognized as very intense at 20.84 Å and 26.51 Å, indicating the importance of the silica or quartz present [16] [17].

After heating, peaks were observed at around 8.64 Å, 17.98 Å, and 26.51 Å, attributed to the interlayered clay minerals montmorillonite-chlorite.

Heat treatment at 550 °C transformed magnetite (Fe₃O₄) into hematite (Fe₂O₃) [18].

Diffraction peaks at around 8.76 Å and 27.44 Å are not displaced during

glycolation, confirming the presence of muscovite-illite. After heating to 550 °C, illite and microcline diffraction peaks at 8.71 Å and 27.78 Å can be observed. The increase in intensity of the microcline diffraction peak at 26.51 Å is further evidence of the presence of microcline [19] [20].

In summary, the glycolation of AKKE clay showed weak sepiolite and anorthite peaks.

Figures 3 and 4 show diffractograms of the three clay samples treated with ethyl glycerol and thermolysis respectively.

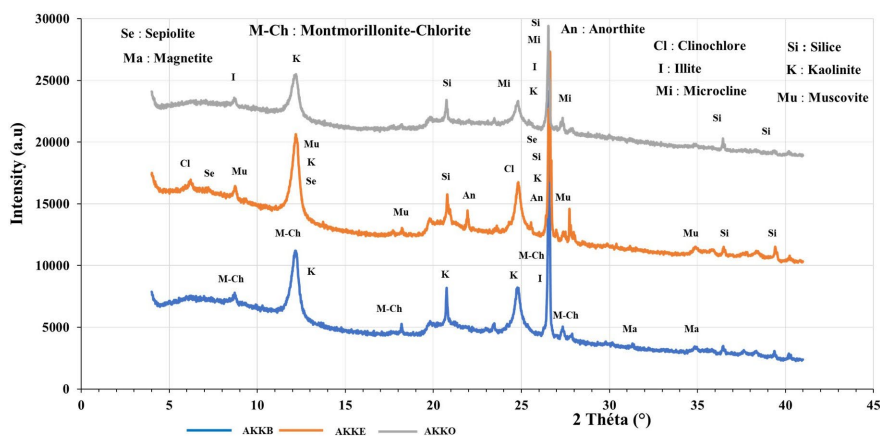


Figure 3. Diffractograms of glycerol-treated Kankan clays.

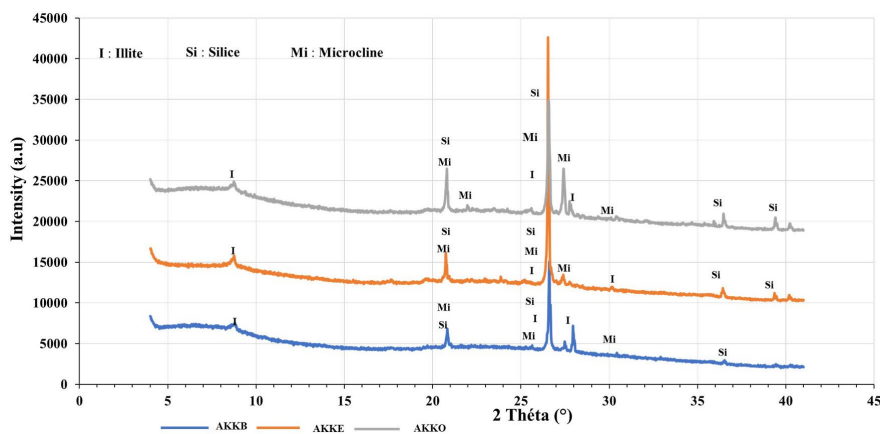


Figure 4. Diffractograms of Kankan clays after thermolysis.

3.1.2. Microstructural Characterization

SEM images of the clays (AKKB, AKKE and AKKO), are shown in Figures 5, 6 and 7 respectively, reveal pseudo-hexagonal plates characteristic of kaolinite, as well as flaky lamellae or aggregates containing cavities [21] [22]. These structures show various alterations depending on the degree of crystallinity, typical of kaolinite [23] [24].

The samples also contain illite smectite, characterized by long, continuous, wavy structures [25].

SEM images suggest that montmorillonite forms an edge-to-edge and edge-to-

face contact structure, while kaolinite and illite platelets are mainly associated in a face-to-face mode [26].

They show the presence of muscovite in the form of flakes [27].

In addition, a significant quantity of grains, probably quartz, is observed. This mineral constitutes impurities, such as the magnetite detected by XRD in sample AKKO [22].

Figures 5, 6 and 7 show scanning electron microscopy images of the AKKB, AKKE and AKKO clays respectively.

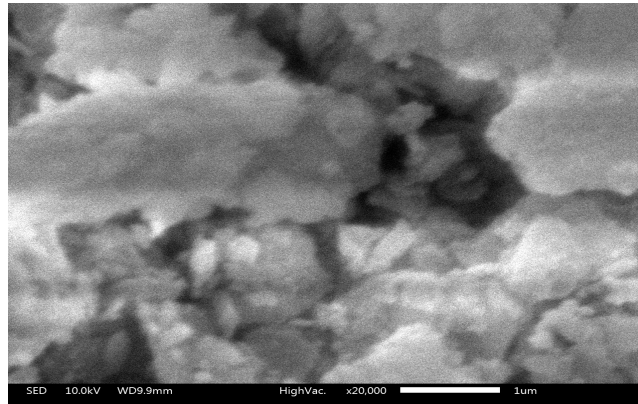


Figure 5. Scanning electron microscopy image of some AKKB clay seeds.

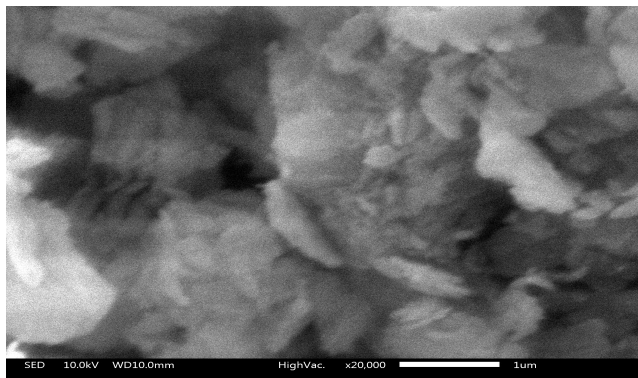


Figure 6. Scanning electron microscopy image of some AKKE clay seeds.

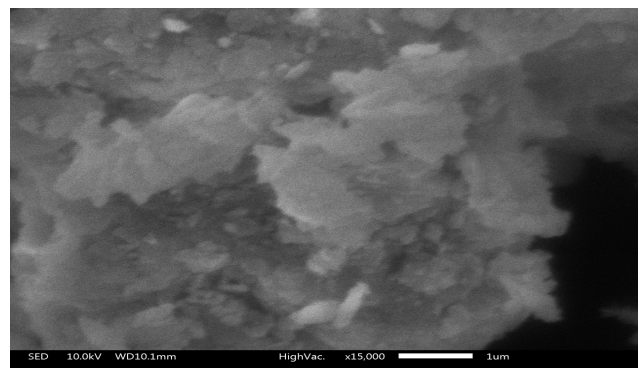


Figure 7. Scanning electron microscopy image of some AKKO clay seeds.

3.2. Elemental Chemical Composition

X-ray fluorescence spectrometry analyses of the AKKB, AKKE, and AKKO clay samples quantified the major chemical elements, in the form of oxides, which are shown in **Table 2**. The three samples are mainly composed of silicon oxide (SiO_2), aluminum oxide (Al_2O_3), iron oxide (Fe_2O_3) and potassium oxide (K_2O).

The mass contents of SiO_2 are 61.62%, 56.91%, and 66.42% respectively, while those of Al_2O_3 are 18.83%, 22.91%, and 19.23%, giving $\text{SiO}_2/\text{Al}_2\text{O}_3$ mass ratios of 3.27, 2.61 and 3.45 respectively. The high $\text{SiO}_2/\text{Al}_2\text{O}_3$ ratios suggest the possible presence of free quartz in a significant proportion within the clay fraction (Gourouza *et al.*, 2013) and/or compounds such as 2/1 clay minerals like illite and muscovite (Coulibaly *et al.*, 2020).

The alumina/silica ratio provides information on the material's permeability to moisture. The higher the ratio, the greater the permeability, indicating that our samples are less permeable [28].

From an industrial standpoint, the $\text{Al}_2\text{O}_3/\text{Fe}_2\text{O}_3$ mass ratio could be used to define the use of clays in the formulation of ceramic bodies. The $\text{Al}_2\text{O}_3/\text{Fe}_2\text{O}_3$ mass ratio of AKKB, AKKE and AKKO clays is less than 5.5, indicating that these clays are rich in iron and would be better suited to the manufacture of building materials (bricks, tiles, etc.) [29].

Loss of ignition is surely due to silicate dehydroxylation reactions, and organic matter combustion (Eliche-Quesada *et al.*, 2018), however, it varies from (6.89% to 9.43%) [30].

Table 2 shows the elemental chemical analysis of the three clay samples.

Table 2. Chemical composition of the raw clay samples.

Oxides	Samples		
	AKKB	AKKE	AKKO
SiO₂	61.62	56.91	66.42
Al₂O₃	18.83	22.91	19.23
Fe₂O₃	7.08	6.93	3.61
K₂O	1.81	1.51	1.83
TiO₂	1.12	1.20	1.08
CaO	0.47	0.33	0.42
LOI	8.33	9.43	6.89
Total	99.26	99.22	99.48
SiO ₂ /Al ₂ O ₃	3.27	2.61	3.45
Al ₂ O ₃ /Fe ₂ O ₃	2.65	3.30	5.32

The chemical analysis of the major elements in the form of oxides in the clay materials also enabled us to identify, from the Augustinik diagram of chemical composition (**Figure 8**), the different areas of use of our raw materials in the manufacture of ceramic products.

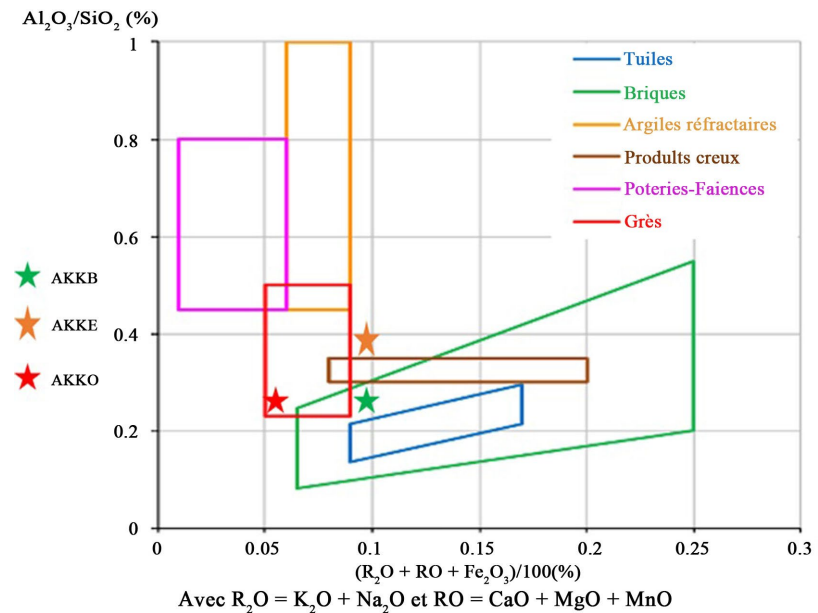


Figure 8. Positioning of the clays studied on the Augustinik diagram.

The location of the samples in this diagram aptly describes the deficiencies in alkaline and alkaline-earth elements, especially for the AKKE clay. For industrial use in traditional ceramics, it would therefore be necessary to consider the addition of compounds rich in melting oxides to facilitate consolidation through the development of viscous flows.

3.3. FTIR Infrared Spectroscopy

The absorption bands located in the high-frequency regions appearing at 3693, 3655 and 3620 cm^{-1} are related to the vibrations of OH hydroxyl groups in kaolinite. The first two bands are respectively attributed to the symmetrical stretching vibrations of the internal surface OH groups and the stretching vibrations of the out-of-plane OH groups. Whereas the band at 3620 cm^{-1} is related to the stretching vibrations of the internal OH groups of kaolinite [31]. The sharp absorption band at 1633 cm^{-1} , attributed to the deformation vibration of H-O-H [31], and the absence of the elongation vibration at around 3400 cm^{-1} point to the low water content of our samples.

The absorption bands at 1114 and 1000 cm^{-1} represent asymmetric and symmetric stretching of Si-O groups, while the bands around 900 cm^{-1} (945 and 911 cm^{-1}) correspond to the deformation of the Al-OH bond in kaolinite [32].

The presence of kaolinite and muscovite can be confirmed by the stretched Si-O bands at 1113 cm^{-1} and 1040 cm^{-1} respectively (Vedder, 1964; Kristof *et al.*, 1993) [17].

The simultaneous presence of bands at 3620 and 910 cm^{-1} indicates that smectite is dioctahedral (Borchardt, 1977). According to Van Olphen and Fripiat (Van Olphen and Fripiat, 1979), the band near 750 cm^{-1} indicates the presence of illite. These results concur with those of the XRD. They confirm the presence of

montmorillonite, kaolinite, and illite in the clay studied [33].

Bands close to 831 and 795 cm^{-1} are attributed to Al-Mg-OH and Si-O-Si bending vibrations respectively and indicate the presence of smectite (Farmer, 1974; Arab *et al.*, 2015). The bands near 777 cm^{-1} have been assigned to the Si-O stretching vibration of quartz (Madejová, 2003; Madejová *et al.*, 2011) [34].

The broad OH extension band near 3625 cm^{-1} , down to less than 3620 cm^{-1} in some cases, coupled with the 825, 750 cm^{-1} doublet (820 and 750 cm^{-1} for our case) confirms the presence of illite [35].

Figure 9 shows the infrared spectra of the three Kankan clays.

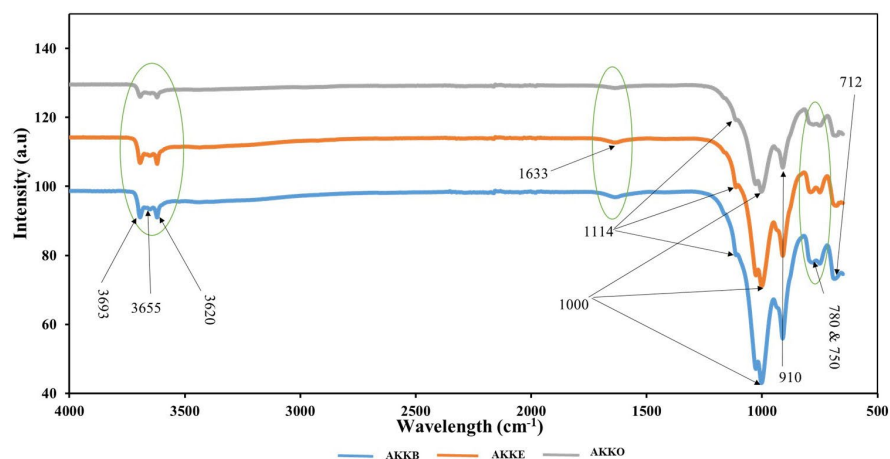


Figure 9. FT-IR spectra of Kankan raw clays.

3.4. Thermogravimetric and Differential Thermal Analysis

Figure 10 shows the ATG/ATD curves for Kankan clays (AKKB - AKKE - AKKO). The ATG curves show three levels of mass loss corresponding to three endothermic peaks at the level of the ATD curves.

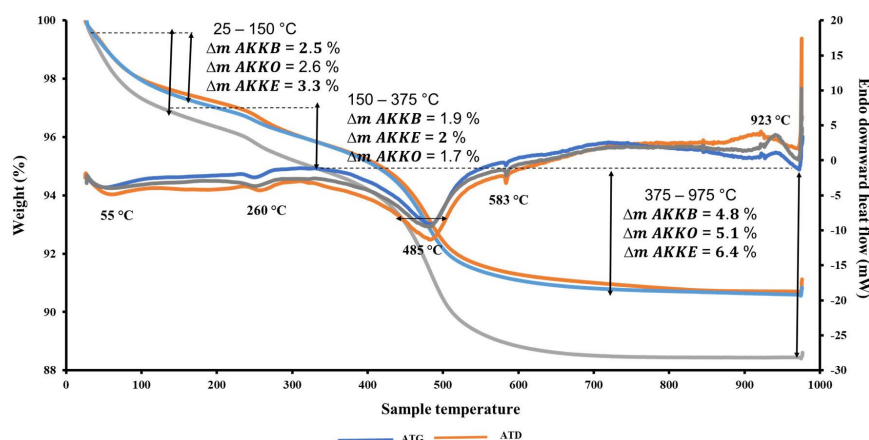


Figure 10. ATG/ATD curves of Kankan raw clays (AKKB - AKKE - AKKO).

The nature of the peak, the mass losses and the physicochemical phenomena responsible for these transformations are summarized in **Table 3**.

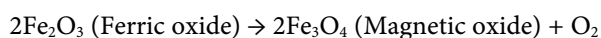
Table 3. Nature of peaks, mass loss and physicochemical phenomena in clays.

Nature of pic	Loss of mass (%)			Comments	
	AKKB	AKKE	AKKO		
Endo (55°C)	2.5	2.6	3.3	(Moisture water discharge)	Moisture water discharge
Endo (260°C)	1.9	1.7	2	(Organic matter decomposition, iron oxidation)	
Endo (485°C)	4.8	5.1	6.4	(Dehydroxylation of kaolinite)	
Endo (573°C)	-	-	-	Transformation quartz α into quartz β	
Exo (923°C)	-	-	-	Recrystallization phenomena	

For the AKKB, AKKE and AKKO clays (**Table 3**), we observe 4 endothermic peaks and 1 exothermic peak. The first endothermic peak, at 55°C, corresponds to the departure of moisture water, accompanied by a loss of mass varying from 2.5% to 3.3%. The second peak at 260°C reflects the loss of inter-foliar water, the transformation of iron oxide and/or organic matter resulting in a mass loss of around 2% [36].

Montmorillonite shows an initial endothermic peak at a temperature of between 100 and 250°C due to the loss of water retained between the basal planes of the lattice structure [37].

An (OH) component is released from the mineral at temperature between 260 and 400°C, where the conversion of Fe₂O₃ to Fe₃O₄ occurs after the hydroxylation process. The phenomenon is observed in the AKKO sample, which contains magnetite according to XRD [38].



The endothermic peak at 485°C is characteristic of the elimination of the constitutive water resulting from the release of hydroxides belonging to the kaolinite lattice according to the following equation $\text{Al}_2\text{Si}_2\text{O}_5(\text{OH})_4 \rightarrow \text{Al}_2\text{Si}_2\text{O}_7 + 2\text{H}_2\text{O}$ (Hajjaji *et al.*, 2001; Bennadji *et al.*, 2008 and Ozkan *et al.*, 2010) [39].

This phase is accompanied by a mass loss of between 4.8% and 6.4%. This event can be attributed mainly to kaolinite dehydroxylation, although illite dehydroxylation may also make a minor contribution [40].

A weak hook at 573°C was noted, highlighting the transformation of α -quartz into β -quartz [41]. Finally, an exothermic peak at 923°C corresponds to the formation of mullite, pseudo-mullite, spinel, amorphous silica, and γ -Al₂O₃ (Földvári, 2011) [42].

3.5. Geotechnical Analyses

3.5.1. Moisture Content

The moisture content of a clay sample is the water content present in the clay as found in its natural state, before any treatment or drying, expressed as a percentage

of the dry weight of the clay. The moisture content of the three clay samples is shown in **Table 4**.

Table 4. Moisture content of Kankan raw clays.

Parameter	Samples		
	AKKB	AKKE	AKKO
Humidity (%)	4.91	7.17	12.10

The water content of Kankan clays (AKKB, AKKE, and AKKO) is 4.91, 7.17, and 12.10 respectively. These low values, compared with the literature, are explained by the low natural permeability of the raw materials, and remain below the water content of pure kaolinitic clay (14%) [43].

3.5.2. Particle Size Analysis

Granulometric analysis consists of determining the size distribution of the grains making up a granulate. The results of particle size analysis are presented in **Table 5**.

Table 5. Particle size distribution of Kankan raw clays.

Particle size	Samples		
	AKKB	AKKE	AKKO
Clay (%)	25.9	23.1	20.0
Sand (%)	21.14	23.3	17.3
Silt (%)	52.6	51.2	62.7

Figures 11, 12 and 13 show the grain size distribution of samples AKKB, AKKE and AKKO respectively.

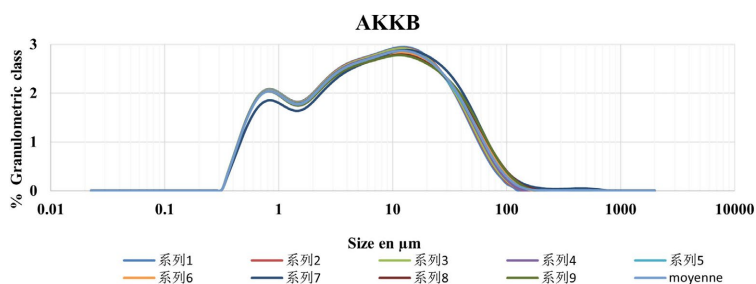


Figure 11. Grain size distribution of AKKB sample showing a bimodal pattern.

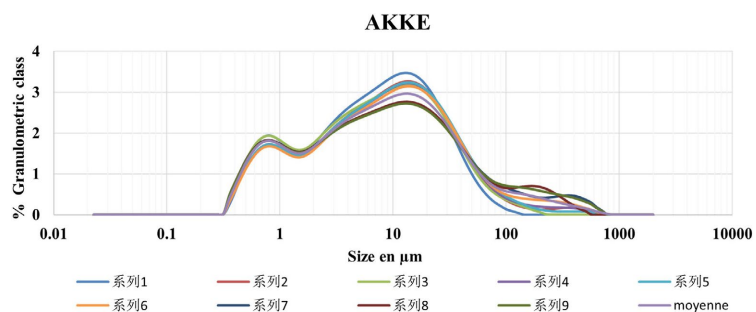


Figure 12. Grain size distribution of AKKE sample showing a bimodal pattern.

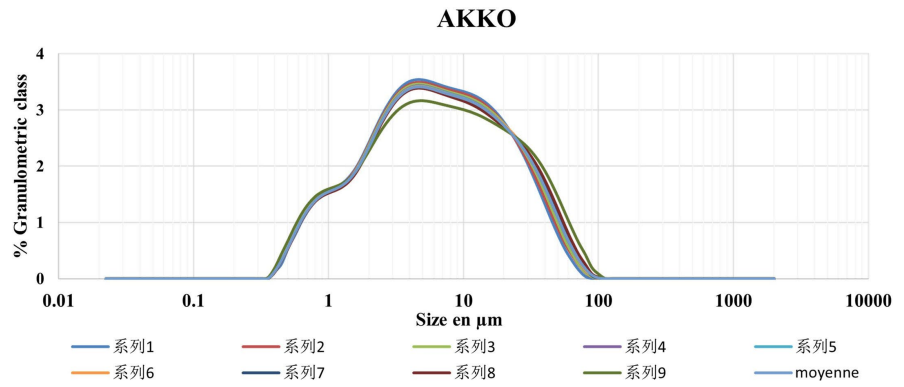


Figure 13. Grain size distribution of AKKO sample showing a Unimodal pattern.

The particle size analyses show:

- An overall bimodal distribution, *i.e.* only the two most important fractions, silt and clay, appear, as shown in figures 2 and 3 for samples AKKB and AKKE. The respective percentages of silt (2 - 20 μm) are 52.6% and 51.2%, while the percentages of clay (0 - 2 μm) are relatively low, at 25.9% and 23.1% respectively.
- Clay and silt fractions are present in over 82.7%, while the sand fraction represents only a small proportion (17.3%), justifying the unimodal distribution of the particle size curves obtained in the case of the AKKO sample.

The GL shows that our samples are less rich in clay fraction (19.6% - 32.8%), but rich in silt fraction (41.8% - 64.2%). This observation is consistent with the particle size classification of ceramic raw materials from Cameroon, Morocco, and Turkey [44]. The predominance of silt-sized fractions (including quartz and feldspar grains) explains why the materials can contribute positively to the clay body skeleton, glass formation, and lowering of vitrification temperature [45].

Evaluation of the three clays on the basis of average grain size was carried out using a Winkler diagram shown in **Figure 14**.

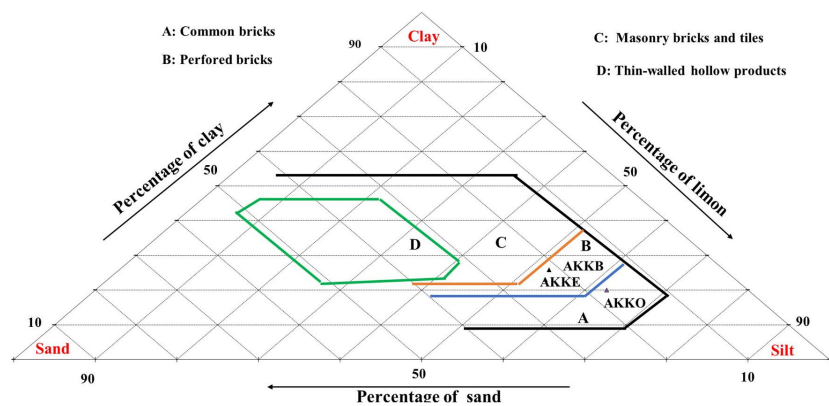


Figure 14. Texture triangle and Winkler diagram of Kankan clays (Dondi, Fannri, and Guarini 1998).

The projection indicates the clays’ suitability for the production of perforated bricks (AKKB and AKKE) and common bricks (AKKO) (Winkler, 1954; Dondi

et al., 1998; Boussen *et al.*, 2016) [46].

3.5.3. Specific Surface Area

The specific surface area of clays is a measure of the total surface area available per unit mass of clay. It includes the external surfaces of particles as well as the internal surfaces of pores and interstices. The specific surface areas of the samples are shown in the table below.

The specific surface of Kankan clays is 23.22 m²/g (AKKO), 30.29 m²/g (AKKB) and 33.48 m²/g (AKKE). According to these specific surface values, AKKO seems to contain less illite and smectite. In general, the specific surface area of kaolinite is generally between (10 - 30 m²/g), and that of illite (80 - 100 m²/g); values around 750 - 800 m²/g are observed for pure smectite [47] [33].

The AKKO clay sample has a lower specific surface area than AKKB and AKKE. Total specific surface area is influenced, among other things, by particle size: the greater the quantity of fine particles, the greater the increase in specific surface area. According to the literature, we can conclude that AKKO contains kaolinite, as its specific surface area is between 10 and 30 m²/g. This is in agreement with the results of the particle size distribution, where the fine fraction (<2 μm) is less important (20%) for AKKO [48].

The mean pore diameter equals 3.8 nm, ranging from 2 to 50 nm, showing that Kankan clays belong to the IUPAC mesopore class (Figure 15).

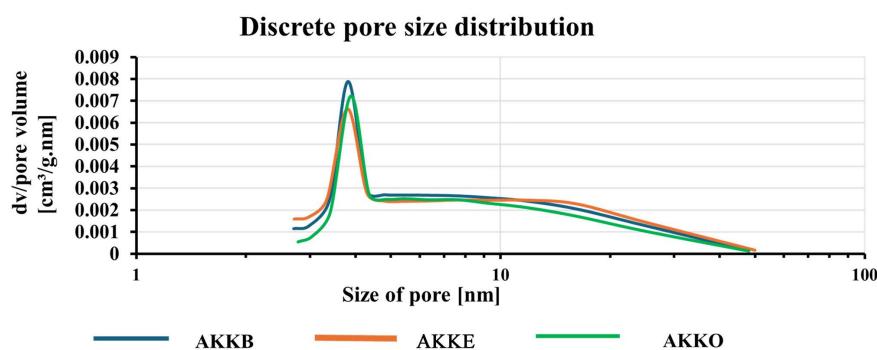


Figure 15. Discrete pore size distribution of Kankan raw clays.

The Brunauer, Emmett, and Teller (BET) method is one of the most commonly used techniques for measuring the specific surface area of materials, applying nitrogen adsorption-desorption at its boiling point of 77° K [49].

According to the classification of the International Union of Pure and Applied Chemistry (IUPAC), the three clays show isotherms similar to type IV isotherms (Figure 16). These isotherms show a hysteresis loop and an adsorption limit in the high relative pressure region. The hysteresis loop is of type H3, indicating the presence of slit-shaped pores [50].

These types of curves exhibit three characteristic pressure intervals: (1) a rapid increase in the amount of gas adsorbed at relatively low pressure (< 0.10), (2) a stable increase at medium relative pressure (0.10 - 0.90), and (3) a sudden increase

at high relative pressure [51].

The notable feature observed in many hysteresis patterns is the forced closure of the desorption branch, where the isotherm “closes” at relative pressures P/P0 around 0.45 - 0.50 for N₂ isotherms, as illustrated by our **Figure 16** [51] [52].

Furthermore, the N₂ adsorption isotherms of our samples do not show a steep initial portion at low relative pressure, indicating a low presence of micropores (< 2 nm) (Deng *et al.*, 2017) [53]. The shape of the isotherms gives a qualitative assessment of the porous structure of the materials [54].

In summary, the profile of isotherms and their hysteresis loops indicate that clays have a porous structure mainly composed of mesopores. This type of pore is characteristic of the lamellar structure of clays [50].

The nitrogen adsorption-desorption isotherms for the three clays are shown in **Figure 16**.

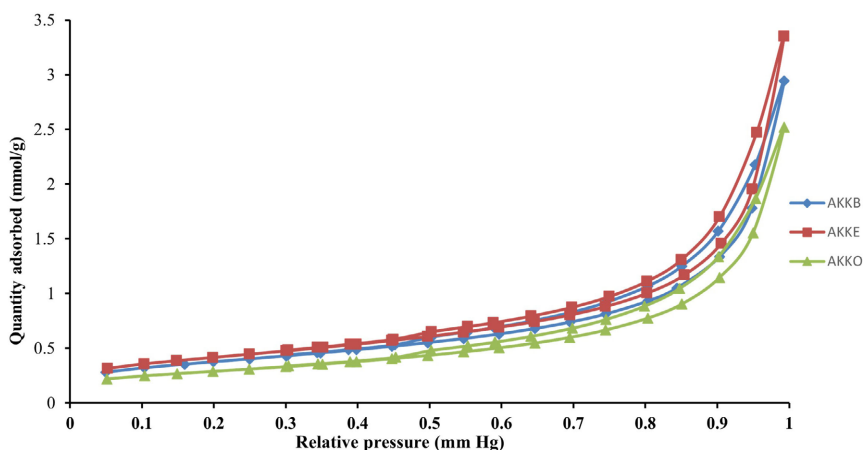


Figure 16. Adsorption and desorption isotherms for Kankan clays.

3.5.4. Plasticity Index

The plasticity index ($IP = LL - LP$) specifies the numerical difference between the Atterberg liquid limit (LL) and the Atterberg plastic limit (LP). Expressed as a percentage of the dry weight of a soil sample, it indicates the range of water contents between which the soil remains plastic. The Atterberg limits for clays are given in **Table 6**.

Table 6. Atterberg limits for Kankan clays.

Atterberg limits (%)	Samples		
	AKKB	AKKE	AKKO
Liquidity limit	45.03	50.22	39.08
Plasticity limit	26.88	26.08	27.01
Plasticity index	18.15	24.14	12.07
Consistncy index	2.39	1.87	3.13

The plasticity limits (LP) of samples AKKB, AKKE, and AKKO lie between 26.08 and 27.01%, and their liquidity limits (LL) are between 39.08% and 50.22%.

The plasticity index (PI) is in the range (12.07% - 24.14%); and the consistency index between (1.87% and 3.13%). The PI of clay samples between 12% and 25% shows that they are not very plastic.

According to Abdelmalek *et al.* (2017), the differences in the plasticity of the samples studied can be explained mainly by the nature of the particle size distribution. These relatively low plasticity index values are directly related to the clay content of our samples.

According to Abdelmalek *et al.* (2017), other factors can affect plasticity properties, such as geological formation, the presence of impurities (*i.e.* non-clay minerals), and organic matter [55]. The plasticity index of our samples is lower than Turkish clay (31% - 33%) (Celik, 2010), and high compared to Brazilia clay (6.5% - 9.8%) (Azzi *et al.*, 2018), Ngaye alluvial clay in Cameroon (9.8% - 20.8%) (Fadil-Djenabou *et al.*, 2015).

Plasticity indices between 5% and 30% confirm the presence of kaolinite in our samples [29]. These results are in line with the range defined in the literature for ceramic production (Célic, 2010; Dondi *et al.*, 2014; Boussem *et al.*, 2016; Mahmoud *et al.*, 2017).

4. Conclusions

The Kankan clays studied display promising characteristics for fabricating construction materials.

The results of mineralogical, physicochemical, geotechnical, and structural characterization of these samples revealed the presence of kaolinite, illite, and montmorillonite, as well as quartz. Clinocllore, muscovite, microcline, gibbsite, and magnetite are also present. Quartz and alumina act as natural binders. Alkalis and alkaline earth are present in small quantities (around 1%), classifying these clays as sandy-clay soils with low plasticity.

According to the Winkler diagram, these clays are suitable for the production of perforated bricks (AKKB and AKKE) and common bricks (AKKO). The location of the samples on the Augustinik diagram clearly shows the deficiencies in alkaline and alkaline-earth elements, especially for the AKKE clay.

The silica-alumina (2.61 - 3.45) and alumina-iron oxide (2.65 - 5.32) ratios not only provide information on the moisture permeability of the raw materials, but also indicate the possibility of their use in the manufacture of building materials (bricks, tiles). The specific surface shows type IV isotherms indicating that the clays possess a mesoporous structure, which has important implications for their adsorption properties and industrial applications. The presence of mesopores and the associated hysteresis loop show a significant capacity to adsorb and retain molecules, which can be useful in many chemical and environmental processes.

The plasticity limits (LP) of samples AKKB, AKKE, and AKKO range from 26.08% to 27.01%, and their liquidity limits (LL) from 39.08% to 50.22%. The relatively low plasticity index of the clay samples (12.07% to 24.14%) shows that they are not very plastic, which is linked to the particle size distribution.

On the basis of their mineralogical, particle size and chemical composition, as well as their geotechnical properties, our clays offer promising potential for use in eco-construction. However, specific additions may be required to optimize their performance, as suggested by Augustinik's figure.

5. Perspectives

This study opens up new perspectives highlighting the potential of the clays studied for effective exploitation in the construction and environmental fields:

- Carry out tests on the mechanical and thermal resistance and carbon footprint of natural and stabilized materials, which will be the subject of the next publication.
- Exploit these clays for the manufacture of perforated bricks (AKKB and AKKE), common bricks (AKKO), and roof tiles, taking advantage of their mineralogical composition and silica-alumina and alumina-iron oxide ratios.
- Studying mesoporous clays for use in pollutant management and the creation of geotechnical barriers in environmental projects.

Conflicts of Interest

The authors declare no conflicts of interest regarding the publication of this paper.

References

- [1] Bergaya, F. and Lagaly, G. (2006) Chapter 1. General Introduction: Clays, Clay Minerals, and Clay Science. In: *Developments in Clay Science*, Elsevier, 1-18. [https://doi.org/10.1016/s1572-4352\(05\)01001-9](https://doi.org/10.1016/s1572-4352(05)01001-9)
- [2] Belghazdis, M., Hachem, E. and Bendouch, A. (2022) Natural Clays from Morocco: Potentials and Applications. *Journal of Sustainability Science and Management*, **17**, 240-254. <https://doi.org/10.46754/jssm.2022.02.017>
- [3] Guggenheim, S. and Martin, R.T. (1995) Definition of Clay and Clay Mineral: Joint Report of the Aipea Nomenclature and CMS Nomenclature Committees. *Clays and Clay Minerals*, **43**, 255-256. <https://doi.org/10.1346/ccmn.1995.0430213>
- [4] Oumar, K.O., Gilbert François, N.N., Bertrand, M.M., Nathanael, T., Constantin, B.E., Simon, M.J., *et al.* (2022) Mineralogical, Geochemical Characterization and Physicochemical Properties of Kaolinitic Clays of the Eastern Part of the Douala Sub-Basin, Cameroon, Central Africa. *Applied Sciences*, **12**, Article No. 9143. <https://doi.org/10.3390/app12189143>
- [5] Kouakou, L.P.M.-., Kouamé, A.N., Doubi, B.I.H.G., Méité, N., Kangah, J.T., Zokou, E.P., *et al.* (2022) Characterization of Two Clay Raw Materials from Côte D'ivoire with a View to Enhancing Them in Eco-Construction. *Journal of Minerals and Materials Characterization and Engineering*, **10**, 198-208. <https://doi.org/10.4236/jmmce.2022.102016>
- [6] Yaya, B.M., Diaka, S., Bakam, S. and Phillippe, B. (2023) Potential Applications of Débéle Clays (Guinea): Formulation of Ceramic Compositions and Hydraulic Binders. *Journal of Natural Sciences*, **3**, 237-247.
- [7] Nshimiyimana, P., Fagel, N., Messan, A., Wetschondo, D.O. and Courard, L. (2020) Physico-Chemical and Mineralogical Characterization of Clay Materials Suitable for Production of Stabilized Compressed Earth Blocks. *Construction and Building Materials*,

- 241, Article ID: 118097. <https://doi.org/10.1016/j.conbuildmat.2020.118097>
- [8] Boufeev, Y.M., *et al.* (2010) Liés; Min. des Mines et de la Géologie Rép. de Guinée; Geoprospects Ltd; Univ. D'Etat de Moscou Lomonossov (Fac. Géol.)-Cona-kry-Moscow; Aquarel.
- [9] ONU-HABITAT (2020) Diagnostic du développement urbain, de la mise en oeuvre des politiques publiques et des défis de l'urbanisation durable en Guinée.
- [10] Barry, T.A. (2023) DATU 2022, Google Earth Projection WGS 84 UTM 29 N.
- [11] Diallo, I.D., Tilioua, A., Darraz, C., Alali, A. and Sidibe, D. (2023) Study and Analysis of Seasonal Soil Degradation in Lower Guinea and Forest Guinea. *Results in Engineering*, **19**, Article ID: 101381. <https://doi.org/10.1016/j.rineng.2023.101381>
- [12] Tchokpon, K.G., Kaki, C., Adissin, G.L., Yessoufou, S. and Kourouma, M. (2019) Metasediments in the Alahina Sector and Associated Mineralization (North-Eastern Guinea). *Open Journal of Geology*, **9**, 897-918. <https://doi.org/10.4236/ojg.2019.912097>
- [13] Diallo, M.-O., *et al.* (2024) Geological Features of the Silakoro (Kintinian) Gold Deposit, SAG Concession-Siguiri Prefecture-Kankan-Guinea Administrative Region. *World Journal of Advanced Research and Reviews*, **21**, 843-857. <https://doi.org/10.30574/wjarr.2024.21.1.2663>
- [14] Vieira, C.M.F., Sánchez, R. and Monteiro, S.N. (2008) Characteristics of Clays and Properties of Building Ceramics in the State of Rio De Janeiro, Brazil. *Construction and Building Materials*, **22**, 781-787. <https://doi.org/10.1016/j.conbuildmat.2007.01.006>
- [15] Danish, A., Totiç, E., Bayram, M., Sütçü, M., Gencil, O., Erdoğan, E., *et al.* (2022) Assessment of Mineralogical Characteristics of Clays and the Effect of Waste Materials on Their Index Properties for the Production of Bricks. *Materials*, **15**, Article No. 8908. <https://doi.org/10.3390/ma15248908>
- [16] Refaey, Y., Jansen, B., El-Shater, A., El-Haddad, A. and Kalbitz, K. (2015) Clay Minerals of Pliocene Deposits and Their Potential Use for the Purification of Polluted Wastewater in the Sohag Area, Egypt. *Geoderma Regional*, **5**, 215-225. <https://doi.org/10.1016/j.geodrs.2015.08.002>
- [17] El-Shater, A. (2022) Crystallographic and Morphological Characteristics of Natural Kaolins, Aswan Region, Egypt. *International Journal of Earth Science and Geology*, **4**, 121-130. <https://doi.org/10.18689/ijeg-1000116>
- [18] Mohamed, M.S., Amer, S.A.M. and Abdel-Kader, G.A. (2021) Clay Mineralogy in Relation to Geomorphic Aspects in Wadi El-Natroun Depression Soils, Western Deserts, Egypt. *Menoufia Journal of Soil Science*, **6**, 363-375. <https://doi.org/10.21608/mjss.2021.213285>
- [19] Fadil-Djenabou, S., Ndjigui, P. and Mbey, J.A. (2015) Mineralogical and Physico-chemical Characterization of Ngaye Alluvial Clays (Northern Cameroon) and Assessment of Its Suitability in Ceramic Production. *Journal of Asian Ceramic Societies*, **3**, 50-58. <https://doi.org/10.1016/j.jascer.2014.10.008>
- [20] Tsozué, D., Nzeugang, A.N., Mache, J.R., Loweh, S. and Fagel, N. (2017) Mineralogical, Physico-Chemical and Technological Characterization of Clays from Maroua (Far-North, Cameroon) for Use in Ceramic Bricks Production. *Journal of Building Engineering*, **11**, 17-24. <https://doi.org/10.1016/j.jobee.2017.03.008>
- [21] Islam, A., Khan, Z., Hussain, M. and Uddin, M. (2022) Scanning Electron Microscopic Analysis of Clays in the Soils of Lower Atrai Basin of Bangladesh. *Dhaka University Journal of Biological Sciences*, **31**, 105-115.

- <https://doi.org/10.3329/dujbs.v3i1i.57920>
- [22] Bakary Soro, S., Coulibaly, M., Paul Gauly, L., N'Dri, S.R., Sanou, A. and Trokourey, A. (2023) Characterization of Clay Materials from Côte D'ivoire: Possible Application for the Electrochemical Analysis. *Journal of Materials Science Research*, **12**, 51-64. <https://doi.org/10.5539/jmsr.v12n1p51>
- [23] Ihekwe, G.O., Shondo, J.N., Orisekeh, K.I., Kalu-Uka, G.M., Nwuzor, I.C. and Onwualu, A.P. (2020) Characterization of Certain Nigerian Clay Minerals for Water Purification and Other Industrial Applications. *Heliyon*, **6**, e03783. <https://doi.org/10.1016/j.heliyon.2020.e03783>
- [24] Kouadio, L.M., Lebouachera, S.E.I., Blanc, S., Sei, J., Miqueu, C., Pannier, F., *et al.* (2022) Characterization of Clay Materials from Ivory Coast for Their Use as Adsorbents for Wastewater Treatment. *Journal of Minerals and Materials Characterization and Engineering*, **10**, 319-337. <https://doi.org/10.4236/jmmce.2022.104023>
- [25] Di Remigio, G., Rocchi, I. and Zania, V. (2021) Scanning Electron Microscopy and Clay Geomaterials: From Sample Preparation to Fabric Orientation Quantification. *Applied Clay Science*, **214**, Article ID: 106249. <https://doi.org/10.1016/j.clay.2021.106249>
- [26] Chen, L., Zhao, Y., Bai, H., Ai, Z., Chen, P., Hu, Y., *et al.* (2020) Role of Montmorillonite, Kaolinite, or Illite in Pyrite Flotation: Differences in Clay Behavior Based on Their Structures. *Langmuir*, **36**, 10860-10867. <https://doi.org/10.1021/acs.langmuir.0c02073>
- [27] Yao, X., Wu, Y., Jiang, J., Chen, X., Liu, D. and Hu, P. (2019) A Population Pharmacokinetic Study to Accelerate Early Phase Clinical Development for a Novel Drug, Teriflunomide Sodium, to Treat Systemic Lupus Erythematosus. *European Journal of Pharmaceutical Sciences*, **136**, Article ID: 104942. <https://doi.org/10.1016/j.ejps.2019.05.020>
- [28] Kormbaye, D., Mougabe, M., Haroun, A., Jonas, T. and Ngarmaim, N. (2024) Physicochemical, Mineralogical and Geotechnical Characterization of the Earth of the 9th District of the City of Ndjamena in Chad with a View to the Construction of Hydraulic Structures. *International Journal of Advanced Research*, **12**, 224-231. <https://doi.org/10.21474/ijar01/18871>
- [29] Garcia-Valles, M., Alfonso, P., Martínez, S. and Roca, N. (2020) Mineralogical and Thermal Characterization of Kaolinitic Clays from Terra Alta (Catalonia, Spain). *Minerals*, **10**, Article No. 142. <https://doi.org/10.3390/min10020142>
- [30] Zaccaron, A., de Souza Nandi, V., Dal Bó, M., Peterson, M., Angioletto, E. and Bernardin, A.M. (2020) Characterization and Use of Clays and Argillites from the South of Santa Catarina State, Brazil, for the Manufacture of Clay Ceramics. *Clay Minerals*, **55**, 172-183. <https://doi.org/10.1180/clm.2020.23>
- [31] Jozanikohan, G. and Abarghooei, M.N. (2022) The Fourier Transform Infrared Spectroscopy (FTIR) Analysis for the Clay Mineralogy Studies in a Clastic Reservoir. *Journal of Petroleum Exploration and Production Technology*, **12**, 2093-2106. <https://doi.org/10.1007/s13202-021-01449-y>
- [32] Vahur, S., Kiudorv, L., Somelar, P., Cayme, J., Retrato, M.D.C., Remigio, R.J., *et al.* (2021) Quantitative Mineralogical Analysis of Clay-Containing Materials Using ATR-FT-IR Spectroscopy with PLS Method. *Analytical and Bioanalytical Chemistry*, **413**, 6535-6550. <https://doi.org/10.1007/s00216-021-03617-9>
- [33] Gourouza, M., *et al.* (2013) Caractérisation d'une argile mixte du Niger. *African and Malagasy Council for Higher Education*, **1**, 36-37.
- [34] Ndzana, G.M., Huang, L., Wang, J.B. and Zhang, Z.Y. (2018) Characteristics of Clay

- Minerals in Soil Particles from an Argillic Horizon of Alfisol in Central China. *Applied Clay Science*, **151**, 148-156. <https://doi.org/10.1016/j.clay.2017.10.014>
- [35] Wilson, M.J. (1994) *Clay Mineralogy: Spectroscopic and Chemical Determinative Methods*. Springer.
- [36] Ravisankar, R., Naseerutheen, A., Rajalakshmi, A., Raja Annamalai, G. and Chandrasekaran, A. (2014) Application of Thermogravimetry-Differential Thermal Analysis (TG-DTA) Technique to Study the Ancient Potteries from Vellore Dist, Tamilnadu, India. *Spectrochimica Acta Part A: Molecular and Biomolecular Spectroscopy*, **129**, 201-208. <https://doi.org/10.1016/j.saa.2014.02.095>
- [37] Mukasa-Tebandeke, I.Z., Ssebuwufu, P.J.M., Nyanzi, S.A., Schumann, A., Nyakairu, G.W.A., Ntale, M., *et al.* (2015) The Elemental, Mineralogical, IR, DTA and XRD Analyses Characterized Clays and Clay Minerals of Central and Eastern Uganda. *Advances in Materials Physics and Chemistry*, **5**, 67-86. <https://doi.org/10.4236/ampc.2015.52010>
- [38] Milošević, M., Dabić, P., Gulicovski, J., Dodevski, V. and Rosić, M. (2024) Mineralogical Characterization of Raw Clay from Rujište (Serbia) Used in Traditional Pottery Manufacture. *Minerals*, **14**, Article No. 469. <https://doi.org/10.3390/min14050469>
- [39] Chakraborty, A.K. (2014) *Phase Transformation of Kaolinite Clay*. Springer.
- [40] Snellings, R., Almenares Reyes, R., Hanein, T., Irassar, E.F., Kanavaris, F., Maier, M., *et al.* (2022) Paper of RILEM TC 282-CCL: Mineralogical Characterization Methods for Clay Resources Intended for Use as Supplementary Cementitious Material. *Materials and Structures*, **55**, Article No. 149. <https://doi.org/10.1617/s11527-022-01973-1>
- [41] Geng, J. and Sun, Q. (2018) Effects of High Temperature Treatment on Physical-Thermal Properties of Clay. *Thermochimica Acta*, **666**, 148-155. <https://doi.org/10.1016/j.tca.2018.06.018>
- [42] Földvári, M. (2011) Handbook of Thermogravimetric System of Minerals and Its Use in Geological Practice. In: *Occasional Papers of the Geological Institute of Hungary*, No. 213, Geological Inst. of Hungary, 68-70.
- [43] Dewi, R., Agusnar, H., Alfian, Z. and Tamrin, (2018) Characterization of Technical Kaolin Using XRF, SEM, XRD, FTIR and Its Potentials as Industrial Raw Materials. *Journal of Physics: Conference Series*, **1116**, Article ID: 042010. <https://doi.org/10.1088/1742-6596/1116/4/042010>
- [44] Salihu, S.A. and Suleiman, I.Y. (2018) Analyse comparative des caractéristiques physiques et chimiques de gisements d'argiles sélectionnés dans l'État de Kebbi. *Au Nigeria*, **13**, 163-173.
- [45] Diko-Makia, L. and Ligege, R. (2020) Composition and Technological Properties of Clays for Structural Ceramics in Limpopo (South Africa). *Minerals*, **10**, Article No. 700. <https://doi.org/10.3390/min10080700>
- [46] Milošević, M., Logar, M. and Djordjević, B. (2020) Mineralogical Analysis of a Clay Body from Zlakusa, Serbia, Used in the Manufacture of Traditional Pottery. *Clay Minerals*, **55**, 142-149. <https://doi.org/10.1180/clm.2020.20>
- [47] Ferrari, S. and Gualtieri, A. (2006) The Use of Illitic Clays in the Production of Stone-ware Tile Ceramics. *Applied Clay Science*, **32**, 73-81. <https://doi.org/10.1016/j.clay.2005.10.001>
- [48] Hussin, A., Rahman, A.H.A. and Ibrahim, K.Z. (2018) Mineralogy and Geochemistry of Clays from Malaysia and Its Industrial Application. *IOP Conference Series: Earth and Environmental Science*, **212**, Article ID: 012040.

- <https://doi.org/10.1088/1755-1315/212/1/012040>
- [49] Athman, S., Sdiri, A. and Boufatit, M. (2019) Spectroscopic and Mineralogical Characterization of Bentonite Clay (Ghardaïa, Algeria) for Heavy Metals Removal in Aqueous Solutions. *International Journal of Environmental Research*, **14**, 1-14. <https://doi.org/10.1007/s41742-019-00232-6>
- [50] Acevedo, N.I.A., Rocha, M.C.G. and Bertolino, L.C. (2017) Mineralogical Characterization of Natural Clays from Brazilian Southeast Region for Industrial Applications. *Cerâmica*, **63**, 253-262. <https://doi.org/10.1590/0366-69132017633662045>
- [51] Boruah, A., Rasheed, A., Mendhe, V.A. and Ganapathi, S. (2018) Specific Surface Area and Pore Size Distribution in Gas Shales of Raniganj Basin, India. *Journal of Petroleum Exploration and Production Technology*, **9**, 1041-1050. <https://doi.org/10.1007/s13202-018-0583-8>
- [52] Amari, A., Gannouni, H., Khan, M.I., Almesfer, M.K., Elkhaleefa, A.M. and Gannouni, A. (2018) Effect of Structure and Chemical Activation on the Adsorption Properties of Green Clay Minerals for the Removal of Cationic Dye. *Applied Sciences*, **8**, Article No. 2302. <https://doi.org/10.3390/app8112302>
- [53] Feng, D., Li, X., Wang, X., Li, J., Sun, F., Sun, Z., *et al.* (2018) Water Adsorption and Its Impact on the Pore Structure Characteristics of Shale Clay. *Applied Clay Science*, **155**, 126-138. <https://doi.org/10.1016/j.clay.2018.01.017>
- [54] Kuila, U. and Prasad, M. (2013) Specific Surface Area and Pore-Size Distribution in Clays and Shales. *Geophysical Prospecting*, **61**, 341-362. <https://doi.org/10.1111/1365-2478.12028>
- [55] Temga, J.P., Mache, J.R., Madi, A.B., Nguetnkam, J.P. and Bitom, D.L. (2019) Ceramics Applications of Clay in Lake Chad Basin, Central Africa. *Applied Clay Science*, **171**, 118-132. <https://doi.org/10.1016/j.clay.2019.02.003>